Eur. J. Mineral.
2008, **20**, 905–916
Published online June 2008

This paper is dedicated to the memory of Werner Schreyer

Lithium and its isotopes in tourmaline as indicators of the crystallization process in the San Diego County pegmatites, California, USA

JENNIFER S. MALONEY[1,4], PETER I. NABELEK[1,*], MONA-LIZA C. SIRBESCU[2] and RALF HALAMA[3,5]

[1] Department of Geological Sciences, University of Missouri, Columbia, MO 65211, USA
*Corresponding author, e-mail: nabelekp@missouri.edu
[2] Department of Geology, Central Michigan University, Mt. Pleasant MI 48859, USA
[3] Department of Geology, University of Maryland, College Park, MD 20742, USA
[4] Current address: Newfield Exploration Company, 363 N. Sam Houston Parkway, Houston, TX 77060, USA
[5] Current address: Institut für Geowissenschaften, Christian-Albrechts-Universität Kiel, 24098 Kiel, Germany

Abstract: In the lithium-cesium-tantalum-type pegmatite dikes of San Diego County, California, USA, tourmaline is the main reservoir for Li, except in the cores and the pockets of the dikes where other Li-bearing minerals also occur. Tourmaline from three subhorizontal dikes was analyzed for bulk Li concentrations and Li isotope ratios. The bottom portion of each dike includes rhythmically layered aplite called line-rock. Above the aplite is the lower pegmatite zone that crystallized upward whereas the hanging pegmatite zone crystallized downward. The lower and hanging pegmatite zones are joined at the core zone. Pockets that were once fluid-filled occur in the core zone.

Tourmaline in the line-rocks and the upper border zones has 22–70 ppm Li and in the pegmatite zones 53–450 ppm Li. Large tourmaline blades in the cores have 174–663 ppm Li. Elbaite rims on prismatic tourmaline in the pockets have up to 5075 ppm Li. The progressive enrichment in Li from the wall-zones to the pockets is attributed to inward fractional crystallization of the dikes. The line-rock in each dike appears to have crystallized until the melt reached fluid saturation, at which point the melt and the fluid began to unmix to form the pegmatite zones and the pockets. The estimated initial Li concentration in the magma that produced the dikes is ~ 630 ppm. At this low concentration, Li has had much smaller effect on crystallization of the dikes than H_2O.

δ^7Li in tourmaline in the line-rocks, the cores, and the pockets ranges from +11.2 to +16.1 ‰ with no systematic difference between these textural zones. However, in radial tourmalines δ^7Li is > 19 ‰. The very elevated δ^7Li may reflect Li isotope fractionation between the melt and the exsolving fluid at the time of crystallization of these tourmalines, with ^{7}Li preferring the more strongly-bonded occupancy in the silicate melt over a hydrated ion occupancy in the fluid. Alternatively, the elevated δ^7Li may also have been caused by preferential accumulation of the slower-diffusing ^{7}Li ahead of the rapidly-growing radial tourmalines. The overall elevated δ^7Li values of the dikes may have been acquired by Li isotope exchange with wall-rocks during passage of the pegmatite melts from their sources.

Key-words: tourmaline, pegmatites, lithium, isotopes, fractionation.

Introduction

A hallmark of granitic pegmatites are their disequilibrium features such as large variations in crystal size, large radial crystal splays and strong mineralogical, textural, and chemical zoning across dikes. The zoning may including rhythmically crystallized aplitic border zones, pegmatite zones, cores and pockets. The pockets, which typically occur in the cores of dikes, represent the space that was once filled by an accumulated fluid. The proposed processes for crystallization of granitic pegmatites range from closed system fractional crystallization of a hydrous melt (Jahns & Burnham, 1969) to rapid cooling to a glass with subsequent development of the pegmatitic texture by constitutional zone refinement (Morgan & London, 1999). Although open system processes have also been proposed to explain the characteristics of granitic pegmatites, the prevalent view is closed-system crystallization of fluxed melts (Černý, 1991).

Water and other fluxing components such as Li and B are central to most crystallization models of granitic pegmatites and their roles must be understood, especially in view of the recognition that pegmatites can crystallize at temperatures < 400 °C (London, 1986a; Thomas *et al.*, 1988; Morgan & London, 1999; Sirbescu & Nabelek, 2003a, b). The fluxing components may play a critical role in permitting crystallization of pegmatitic melts at very low temperatures, be it by unmixing involving production of a fluxed F, B, and P-rich melt (Thomas & Klemm, 1997; Thomas *et al.*, 2000) or by permitting rapid crystal growth

rates in highly undercooled melts (Webber *et al.*, 1999; Nabelek, 2007; Sirbescu *et al.*, 2008).

This study was inspired in part by the work of Werner Schreyer on the crystal-chemistry of tourmaline. His work has demonstrated the value of tourmaline as an indicator of the petrogenesis of igneous rocks, including pegmatites (*e.g.*, Schreyer *et al.*, 2000; Kalt *et al.*, 2001). In the present study, concentrations and isotopic ratios of Li in tourmaline are used to constrain the role of Li in the crystallization of three pegmatite dikes in the San Diego County, California, USA. These dikes have been studied by many workers including as a foundation for the classic pegmatite crystallization model of Jahns & Burnham (1969). In the lithium-cesium-tantalum (LCT) family of pegmatites, to which the San Diego County dikes belong, Li occurs at concentrations high enough to cause crystallization of Li minerals, including elbaite tourmaline $[Na(Li_{1.5}Al_{1.5})Al_6B_3Si_6O_{27}(OH)_3(OH,F)]$, spodumene $[LiAlSi_2O_6]$, amblygonite-montebrasite $[(Li,Na)AlPO_4(F,OH)]$, and lepidolite along the polylithionite $[KLi_2AlSi_4O_{10}(F,OH)_2]$ – trilithionite $[KLi_{1.5}Al_{1.5}AlSi_3O_{10}(F,OH)_2]$ join (Černý & Ercit, 2005). Because Li can substitute into tourmaline which is ubiquitous in all portions of the San Diego pegmatite dikes, tourmaline was used here as a proxy for determining the behavior of Li and to assess its importance for fluxing granite melts. Isotope ratios of Li can be a mirror on magma differentiation because the fractionation of Li isotopes in a multiphase system is to a large extent controlled by its coordination in coexisting phases and/or kinetics (Wenger & Armbruster, 1991; Richter *et al.*, 2003; Wunder *et al.*, 2006, 2007).

Geologic context and samples

The pegmatites of San Diego County are located within the northwest trending, subduction-related Peninsular Ranges Batholith (PRB) that stretches from the San Jacinto Mountains of California into Baja California, Mexico (Fig. 1). The batholith is divided into the western and eastern zones (Walawender *et al.*, 1990; Fisher, 2002; Todd *et al.*, 2003). The western zone is comprised of I-type gabbros, quartz diorites, tonalites, granodiorites, and monzogranites ranging in age from 120 to 105 Ma in age. The more felsic eastern zone lacks gabbros and is dominated by large, concentrically-zoned I- and S-type tonalites and monzogranites whose intrusion began at ~ 105 Ma when magmatism in the western zone stopped due to a change in plate dynamics. Some of the intrusions include the 100 and 89 Ma La Posta-type plutons that straddle to east-west boundary of the PRB (Walawender *et al.*, 1990; Symons *et al.*, 2003). La Posta-type plutons are zoned inward from hornblende tonalite to muscovite-bearing monzogranite. The pegmatite field is broadly contemporaneous with the La Posta-type plutons and also straddles the east-west boundary. The pegmatites occur as suites of parallel to subhorizontal dikes mostly within the plutons and occasionally within intervening schists. The dikes were emplaced at 2–3 kbar based on densities of fluid inclusions trapped in pockets (London, 1986b). The host plutons appear to have been brittle when the dikes were emplaced.

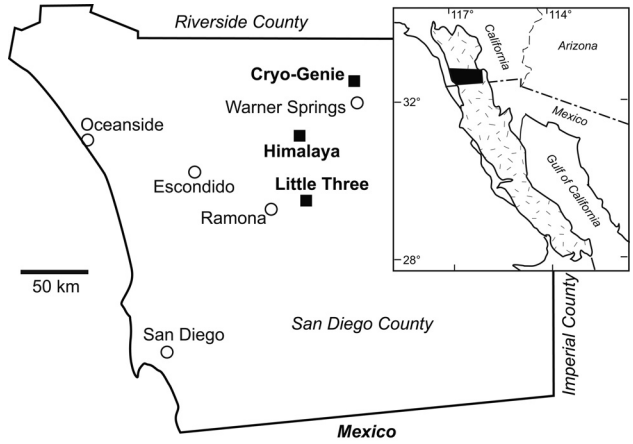

Fig. 1. Regional sketch showing locations of the Cryo-Genie, Little Three, and Himalaya pegmatite dikes in the San Diego County, California. Inset shows location of the Peninsular Ranges Batholith (stippled). The black rectangular shape is San Diego County.

Tourmaline was collected from three pegmatite dike systems – the Cryo-Genie, the Little Three, and the Himalaya (Fig. 1). Dikes in all three systems exhibit similar zoning in mineralogy, texture, and chemistry (Jahns & Tuttle, 1963; Jahns, 1979). A typical dike has a lower border zone that is characterized by rhythmically-layered aplite with oscillating changes in mineralogy from Mg-Fe-poor layers dominated by quartz and albite to Mg-Fe-rich layers dominated by tourmaline and sometimes garnet. This layered aplite is colloquially called "line-rock". Above the line-rock is the lower pegmatite zone with upward growth direction of minerals. The hanging part of the dike is characterized by a thin border zone, which occasionally is also layered. Below this border zone is the hanging pegmatite with large euhedral K-feldspar crystals and then graphic quartz-feldspar intergrowths. Between the hanging and lower pegmatites is the coarse-grained core zone. The core zone includes pockets that have variable size and occurrence along the dike's strike. Aside from gem-quality crystals, the pockets are often partially filled with clays that suggest low-temperature alteration of core and pocket minerals by magmatic fluids (Foord *et al.*, 1986). When pockets are absent, the demarcation between the lower and hanging portions of the dike is shown by opposite growth directions of minerals and occurrences of massive quartz, large amount of mica and large tourmaline blades. In this paper, both a coarse-grained core and a wall of a pocket are referred to as the "core zone".

The main Cryo-Genie dike intruded into sillimanite-grade metasedimentary rocks and a portion of the local La Posta-type granite. Field relationships with dated granites suggest that the dike was emplaced between 98 and 89 Ma (Kampf *et al.*, 2003). The dike is 2–4 m thick and can be traced for more than 200 m. The analyzed samples were collected at the Green Ledge surface excavations and around the Payday pocket in underground excavations (Table 1; Fig. 2a, b). At Green Ledge only the upper portion of

Table 1. Tourmaline locations, shapes and Li concentrations and isotope ratios.

Sample	Zone	Tourmaline shape	Li (ppm)	δ^7Li (‰)
CG-1a	middle hanging pegmatite	radial	53	19.2
CG-1c	core zone	large blade	174	
CG-1e	core zone	large blade	138	
CG-1i black	pocket	prism	273	15.9
CG-1i green	pocket	prism	5075	14.7
CG-1n	pocket	prism	416	11.2
CG-3e	core zone	large blade	265	16.1
CG-3i	core zone	large blade	663	11.2
CG-3k	middle hanging pegmatite	radial	421	
CG-5b	top border	short blade	22	
CG-5d	middle hanging pegmatite	radial	93	
LT-1c	core zone	large blade	517	13.4
LT-3f	bottom line rock	small prismatic	56	15.1
LT-3g	bottom line rock	small prismatic	66	
LT-3i	bottom line rock	small prismatic	70	12.3
LT-4c	core zone	large blade	268	14.8
LT-5c	bottom pegmatite	radial	452	22.9
LT-5d	bottom pegmatite	radial	113	19.1
LT-5e	bottom pegmatite	small prismatic	135	14.2
HM-2C black	pocket	prism	641	15.9
HM-2c green	pocket	prism	1456	13.7
HM-4C	pocket	prism	954	15.9

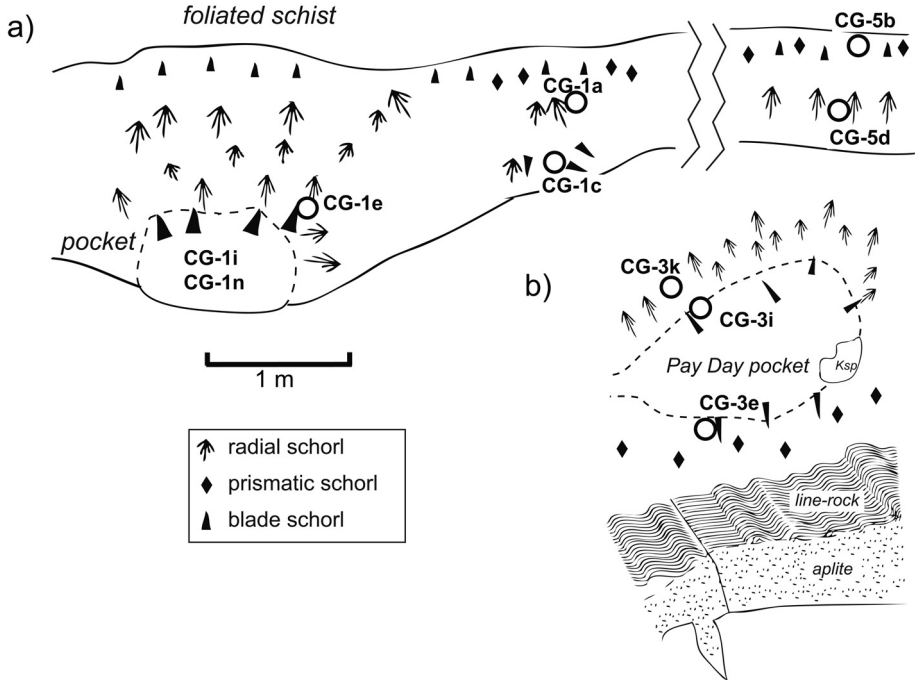

Fig. 2. Sketches showing sample locations at the Cryo-Genie pegmatite dike, (a) Green Ledge location on the surface, and (b) Payday pocket underground.

the dike, from the upper contact to the core zone, including a pocket, is exposed. CG-5b is a short euhedral tourmaline from the border of the hanging pegmatite, CG-1a, and CG-5d are radially-grown tourmaline needles from the hanging pegmatite, and CG-1c and CG-1e are large euhedral tourmalines from the core zone. CG-1i and CG-1n are tourmaline prisms that grew into the pocket. CG-1i has a schorl core and green elbaite rim. CG-3e and CG-3i are schorl blades from core zone around the Payday pocket whereas CG-3k is radial schorl from the pegmatite above the pocket.

The Little Three dike system intrudes the Green Valley tonalite-gabbro of the western zone of the PRB (Stern *et al.*, 1986). The system has five dikes, including the Little Three main dike and the Spaulding dike that were sampled for this study. The dikes vary between 1 and 2 m in thickness along strike. The relative thickness of line-rock and pegmatite zones also varies. Most of the analyzed samples come from the Little Three main dike near the mine entrance on Topaz Ledge (Fig. 3). The bottom boundary of the dike with the country rock is a homogeneous aplite with line-rock above it. The line rock terminates sharply against the lower pegmatite zone which contains small prismatic or bladed tourmaline within graphic intergrowths of quartz and feldspar.

Samples LT-3f, LT-3g and LT-3i come from the line-rock (Fig. 3a). Samples LT-5c and 5d are radial tourmalines that grew in the lower pegmatite that cuts through the line rock along strike from location 3 (Fig. 3b). LT-5e is a prismatic tourmaline in a smaller dike cutting through the line rock. Sample LT-4c is a large tourmaline blade from the core zone around a several-meter size pocket that occurs above the mine entrance. Sample LT-1c is a similar tourmaline from the core zone of the Spaulding dike.

The Himalaya dike system includes two subparallel dikes hosted by the San Marcos gabbro (Fisher *et al.*, 1999; Webber *et al.*, 1999). The two dikes are separated by 3–10 m along the 915 m of their exposed length but converge at the San Diego mine where the samples were collected. The Himalaya dikes were emplaced ~ 100 m.y. ago, as dated by fission track and K-Ar methods (Foord, 1976). Samples HM-2c and HM-4c come from pockets in the underground workings of the San Diego mine. Tourmaline HM-2c includes a schorl core and a green elbaite rim while HM-4c is exclusively schorl.

The Cryo-Genie samples best represent a cross-section across the hanging portion of a pegmatite dike while the Little Three samples best represent the lower portion of a dike. The Himalaya samples were analyzed primarily to determine if there is a regional variability in Li isotopic compositions.

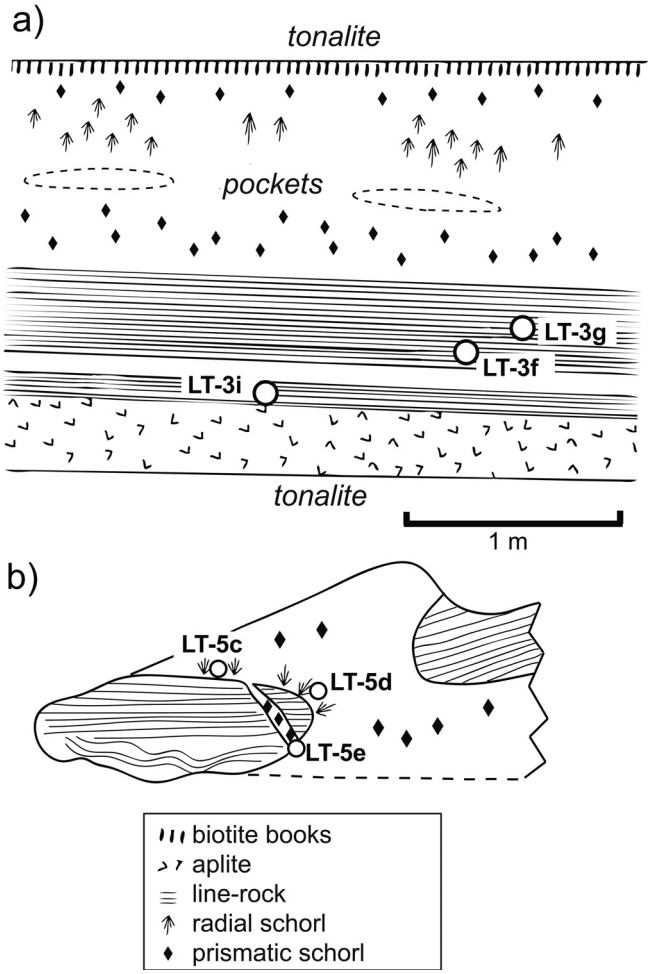

Fig. 3. Sketches showing sample locations at the Little Three pegmatite dike. Parts a) and b) are along strike on the main dike.

Methods

Bulk Li concentrations

Tourmaline is extremely difficult to dissolve in acids, and therefore we have developed a flux procedure that accomplishes complete dissolution of ground-up tourmaline. Black cores and green rims of zoned pocket tourmalines were prepared separately. When samples had only small crystals, multiple grains were ground together. 100 mg of each tourmaline powder were mixed with 400 mg of ground K_2CO_3 flux in a zirconia crucible and placed into a furnace at 500 °C. The temperature was then increased to 900 °C for 15 min, after which the furnace was turned off. The crucibles were left in the furnace overnight to slowly cool to prevent cracking. Each fluxed sample was first centrifuged in 15 ml of 10 % HNO_3 for four minutes. The liquid was then decanted into a Teflon beaker and stirred on a hot plate. The remaining solid residue was again centrifuged in 15 ml of 10 % HNO_3. Any residue that was still left was dissolved in 3 ml of concentrated HNO_3 and was then added to the already dissolved tourmaline and stirred for additional 15 minutes on low heat. The sample was then brought up to 50 ml in a volumetric flask with 10 % HNO_3. In several samples, a brown amorphous precipitate formed after several days. After the liquids were decanted, the precipitates were dissolved in a HF-HNO_3 mixture and then diluted to 50 ml with distilled water. Analysis of these solutions revealed no Li.

Lithium concentrations (Table 1) were analyzed using the Perkin-Elmer Optima 3300 Inductively Coupled Plasma

Optical Emission Spectrometer (ICP-OES) at the University of Missouri. Synthetic standards with 0.05, 0.10, 1, and 5 ppm Li were prepared using blank K_2CO_3 flux solutions to create the calibration curves for Li. Instrumental drift was accounted for by analyzing the prepared standards at regular intervals during the analysis and aliquots of the standard solutions were used as check standards. Lithium concentrations were obtained from the strong 610.362 nm emission line.

Li isotope ratios

Analysis of Li isotope ratios (Table 1) was carried out on dried aliquots of solutions prepared for ICP-OES analysis. The dried samples were prepared and analyzed at the Geochemistry Laboratory of the University of Maryland-College Park. The preparation followed the procedure outlined in Rudnick *et al.* (2004) and Teng *et al.* (2004), which is based on the three-column procedure of Moriguti & Nakumura (1998). Because Na/Li ratio in solution larger than ~ 5 may cause instability in the analysis, the Na/Li ratio of each sample was determined semi-quantitatively prior to analysis, and excess Na was stripped-off by additional column purification. Measurements were done on a Nu Plasma Multicollector Inductively Couple Plasma Mass Spectrometer (MC-ICP-MS). Each analysis consisted of two blocks of twenty individual measurements. Each analysis was bracketed by the measurement of a 100 ppb L-SVEC standard. The $^7Li/^6Li$ ratio in L-SVEC for each 2×20 measurements had an average 2σ of the mean $\leqslant 0.003$. The external precision better than 1 ‰. Two other Li isotope standards, IRMM-016 (Qi *et al.*, 1997) and the in-house standard UMD-1, were routinely analyzed during each analytical session. The results for both (IRMM-016: +0.2 ± 0.4; UMD-1: +54.3 ± 0.2) agree well with published results (IRMM-016: –0.1 ± 0.2 to +0.2 ± 0.8; UMD-1: +54.7 ± 1.0; Rudnick *et al.* 2004; Teng *et al.* 2004; Halama *et al.* 2007). Two USGS rock standards, BHVO-1 (+4.2 ‰) and QLO-1 (+6.6 ‰), were analyzed for quality-control purposes. The value for BHVO-1 was within the uncertainty of previously published results (+4.3 to +5.8; Bouman *et al.* 2004; Rudnick *et al.* 2004), and the value for QLO-1 was within the range of previous analyses at the University of Maryland (+5.6 to +6.8; Halama, unpublished data).

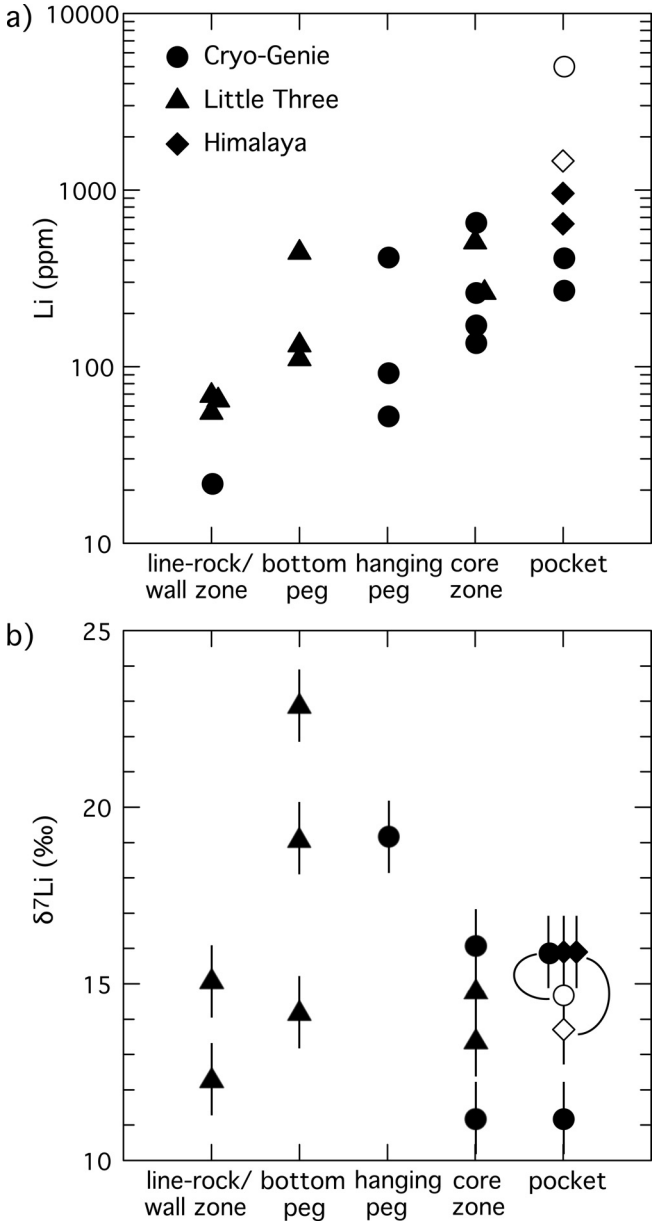

Fig. 4. (a) Li concentrations and (b) Li isotopic ratios in tourmalines in three pegmatite dikes. Data are grouped according to textural zones from which samples came from. Schorl tourmalines are shown by black symbols and elbaite rims on schorl by white symbols. Two core-rim pairs are shown by connecting lines.

Results

Li concentrations

Li concentrations in the tourmalines (Table 1) are shown in Fig. 4a. They are plotted in terms of the zones in which the tourmalines grew. There appear to be no systematic differences in Li concentrations between corresponding zones of the different dikes based on the available data, in spite of the spatial and probably some temporal separation of the dikes, although with denser data sets for all three dikes, some systematic differences could appear. Nevertheless, the similar ranges in Li concentrations in the pegmatite and the core zones of both the Cryo-Genie and the Little Three dikes, for example, point to a common petrogenetic process of the dikes that is underscored by their similar tectonic context, the similar style of emplacement, and the similar textural and mineral zoning across the dikes.

There is a progressive increase of about two orders of magnitude in Li concentrations across the zones of individual dikes. For example, in the Cryo-Genie dike, concentrations range from 22 ppm to 5075 ppm. The lowest Li concentrations, $\leqslant$ 70 ppm, are in tourmalines in the line-rock of the Little Three main dike and the top border zone of the

Cryo-Genie dike. These tourmalines are at most few millimeters in length and are prismatic. Li concentrations in radial tourmalines in the pegmatite zones of both the Cryo-Genie and Little Three dikes and in large tourmaline blades in the core zones are on average higher by about an order of magnitude. The concentrations are highly variable, however. In prismatic schorl crystals within pockets, the concentrations range from 273 to 954 ppm. Two green overgrowths on schorl cores have the highest Li concentrations, 1456 and 5075 ppm.

Li isotope ratios

In contrast to the progressive increase in Li concentrations in tourmalines across the zones of the dikes, the variation in δ^7Li is more complex (Fig. 4b). There is no correlation with Li concentrations, but again, there appears to be no systematic difference in δ^7Li between the three dikes. In tourmalines from the wall-zone/line-rock, core zone and pockets, δ^7Li has approximately the same range, between 11.2 and 16.1 ‰. In the pockets, elbaite rims have lighter Li than schorl cores, although the difference in the Cryo-Genie pair is within overlapping errors. In three tourmalines from the upper and the lower pegmatite zones of both Cryo-Genie and Little Three dikes, δ^7Li is very high, > 19 ‰. These three tourmalines came from radial splays, whereas others with lighter Li were prismatic or blade-shaped (Fig. 3b). δ^7Li in prismatic tourmaline from the bottom pegmatite zone of the Little Three dike is lower at 14.2 ‰.

The obtained δ^7Li values and their range are among the highest measured in rocks. δ^7Li in most unaltered crustal rocks typically does not exceed 10 ‰ (Tomascak, 2004; Teng *et al.*, 2004) but values up to 19 ‰ in quartz and a 10 ‰ difference between quartz and albite have been reported for the Tin Mountain pegmatite in the Black Hills, South Dakota, USA (Teng *et al.*, 2006b).

Initial Li concentration in pegmatite melts

Lithium is often invoked as an element that may contribute to growth of large crystals that characterize pegmatites by depolymerizing the silicate melt structure and therefore lowering its viscosity and increasing chemical diffusion rates. In order to evaluate the fluxing effect of Li compared to H_2O in the San Diego County pegmatites, a crude estimate was made of its initial concentration in the melts. The estimate comes from the Li concentrations in tourmaline, the modal abundance of tourmaline, and the Li concentrations in fluid inclusions in pocket quartz, assuming that the pockets were the collection volumes for the separated fluid. Tourmaline is the largest reservoir for Li in the line rock and pegmatite, but in the cores and pockets where other Li-bearing minerals, including lepidolite and amblygonite occur, Li concentration in the fluid is best estimated from primary fluid inclusions in quartz. In the Little Three pegmatite these inclusions have a range of 7000 to 12 000 ppm with average of 9200 ppm Li (unpublished data determined by ion chromatography). The inclusion fluids contain ~ 3 wt.% NaCl, based on microthermometric measurements.

The initial concentration of Li in the pegmatite melts (C_o) can be estimated using:

$$C_o = X_{LR}C_{LR} + X_{PEG}C_{PEG} + X_{POCK}C_{POCK},$$

where X is the mass proportion of each zone and C is the concentration of Li in each zone. Li concentrations in the line-rock and the pegmatite zones were determined from the average of Li concentrations in tourmaline in each zone and the modal proportions of tourmaline. Data for the Cryo-Genie and Little Three dikes were combined. Combining the data for the two dikes is justified because in the pegmatite zones, which are volumetrically most abundant, Li concentrations cover the same ranges. The average Li concentration in tourmaline in the Cryo-Genie pegmatite zones is 258 ppm and in the Little Three it is 298 ppm. The mass proportions of the three zones were determined from their relative volumes and densities, 2700 kg/m^3 for the rocks and 500 kg/m^3 for the fluid. The fluid density is appropriate for H_2O with 3 wt.% NaCl at 2 kbar and 400 °C (Anderko & Pitzer, 1993). The proportion of tourmaline in the line-rock and pegmatite zones is < 8 volume %, based on image analysis of cut slabs. The estimated bulk Li concentration in the line-rock zones is only ~ 5 ppm and in the pegmatite zones only ~ 60 ppm. It is readily evident that most Li from the original melt ended-up in the fluids.

The pockets show that the exsolved fluid was collected in discrete spaces instead of one continuous space between the hanging and lower portions of the dikes. Because the volume and the distribution of the pockets are highly variable (Jahns, 1979; Stern *et al.*, 1986), the volume of the exsolved fluid is difficult to estimate from the field occurrences of the pockets. A better estimate of the volume of the exsolved fluid comes from the maximum H_2O solubility in silicate melts, which at 2 kbar is ~ 6 wt.% (Holtz *et al.*, 1995). This amount of H_2O, given its molar volume at 400 °C and 2 kbar, would occupy ~ 28 % of the chamber volume. Using this proportion, the calculated initial Li concentration in the pegmatite dikes is only ~ 630 ppm. If the Cryo-Genie data is left out of the calculation, the difference in the result is only 1 ppm. Although the ranges of the measured Li concentrations and errors in the volume estimates of tourmaline and the textural zones contribute to an error on this estimate, the estimate is dominated by the calculated fluid volume and the Li concentration in the fluid as determined from fluid inclusions. Although 630 ppm Li could appear to be a rather small concentration for a LCT-type melt, it is 18 times greater than the estimated average concentration of 35 ppm in the upper continental crust (Teng *et al.*, 2004).

Discussion

Role of lithium in the pegmatite crystallization process

Since the classic model of Jahns & Burnham (1969) for crystallization of pegmatite melts, which involves the

separation of a fluid phase from a silicate melt, it has been recognized that the formation of pegmatites also depends on kinetic controls during rapid cooling of dikes, in particular enrichments of components in melt boundary layers ahead of rapidly crystallizing minerals (*e.g.*, Rockhold *et al.*, 1987; London, 1992; Webber *et al.*, 1999). In addition to being responsible for crystallization of minerals in which it is an essential structural constituent, Li is often invoked as a possible component that, along with H_2O, B, F, and other species, can potentially flux granite melts. For example, fractional crystallization involving Li was partly responsible for mineral zoning seen in the large LCT-type Tin Mountain pegmatite in the Black Hills of South Dakota, in which the outer zones are dominated by feldspars and the inner zones by spodumene and quartz (Walker *et al.*, 1986). Trapping temperatures of primary fluid inclusions are < 400 °C and nearly invariable across the pegmatite, suggesting that it crystallized nearly isothermally as an undercooled liquid (Sirbescu & Nabelek, 2003a).

An extreme kinetic model is that of Morgan & London (1999) for crystallization of the Little Three pegmatite. They suggested that the low temperature and the fast cooling rate that must have occurred during solidification of the pegmatite did not allow for crystal nucleation until the melt has reached a glass state at ~ 250 °C below the equilibrium liquidus. They proposed a constitutional zone-refining process, in which a fluxed crystallization front swept a F, Li, and Mn-rich boundary layer through the solid or semi-solid dike, eventually resulting in enrichment of these elements in the pocket zone.

Although we did not obtain electron microprobe data on tourmaline from the dikes, the electron microprobe data of Morgan and London (1999) on tourmaline in the Little Three dike suggests that the progressive increase in Li concentrations from the line-rock and the upper wall-zone to the pockets (Fig. 4a) corresponds to changes in other tourmaline components. Morgan & London (1999) found that across the line-rock and the pegmatite zones, Mg decreases from ~ 0.7 to near 0 per formula unit while Fe stays nearly constant. The increase in Li and the decrease in Mg suggests an increasing exchange of the elbaite component for the dravite component. In the pockets, tourmaline is zoned from schorl to elbaite but the zoning appears to be continuous without an evidence for a miscibility gap (Morgan & London, 1999), consistent with evidence for complete solid solution between schorl and lithian olenite in a pegmatite from the eastern Alps (Kalt *et al.*, 2001). Elbaite in the pockets has elevated F and Mn concentrations (Morgan & London, 1999). The occurrence of schorl cores in the pockets suggests that schorl grew while Fe-bearing melt was still present in the dikes, but the elbaite rims, together with other lithium minerals in pegmatite cores and pockets, grew in equilibrium with Li-rich fluid collected in the pockets. The progressive increase in Li across the dikes is more consistent with progressive inward crystallization of the dikes than a zone-refining process as Li appears to have been progressively enriched in the residual liquid because of its low solubility in early-crystallizing minerals, including schorl. The change in tourmaline composition across the San Diego County pegmatites is analogous to the tourmaline composition trend in the Bob Ingersol pegmatite in the Black Hills (Jolliff *et al.*, 1986).

The transition from the aplitic line-rock to pegmatite probably marks the point of fluid separation in the magma. Fluid separation is suggested by the occurrences of elongated radial crystals that characterize the pegmatite zones, because crystals grow faster and become elongated when H_2O activity increases in the melt (Fenn, 1977). High H_2O activity promotes an increase in the diffusion rates of chemical components even when the melt is undergoing rapid cooling. Crystallization of tourmaline (and garnet) is controlled more by gradients in concentrations of less mobile elements, including Fe, Mg, and Mn, than by gradients of rapidly-diffusing elements, especially the alkalis (Rockhold *et al.*, 1987; Webber *et al.*, 1999). The lack of crystallization of Li minerals such as spodumene and amblygonite until the core zones was probably precluded by the initially low Li concentration and removal of Li by the exsolving fluid. Although in Cl-absent, water-peraluminous melt systems $D(\mathrm{Li})^{\mathrm{fluid/melt}}$ is ~ 0.4 (London *et al.*, 1988), $D(\mathrm{Li})^{\mathrm{fluid/melt}}$ increases with the addition of Cl. For example, when an aqueous fluid at 800 °C/2 kbar has ~ 7 wt.% Cl, $D(\mathrm{Li})^{\mathrm{fluid/melt}}$ is ~ 2 (Webster *et al.*, 1989). However, even this $D(\mathrm{Li})^{\mathrm{fluid/melt}}$ seems insufficient to explain the very elevated Li in the pocket fluids by simple batch partitioning between the fluid and the melt, particularly because the fluid contained only ~ 2 wt.% Cl. More likely, the large concentration of Li in the fluid is the result of Rayleigh enrichment with crystallization dominated by feldspars, quartz, and schorl tourmaline in which Li has small solubility compared to the melt and the fluid. At 88 % crystallization, Li would have exceeded 0.5 wt.% (1.1 wt.% Li_2O) in the melt and a correspondingly high concentration in the accumulating fluid.

Concentrations in excess of 1 wt.% Li_2O that may have existed at later stages of fractional crystallization of the dikes are approached in some large spodumene-bearing pegmatite intrusions, including the Tin Mountain pegmatite, the Harding pegmatite in New Mexico, and the Tanco pegmatite in Manitoba (Norton, 1994). These large pegmatites contain spodumene and/or other Li-bearing minerals not only in their cores but also other zones (Norton, 1994). Li_2O concentrations approaching 1 wt.% in a silicate melt may be required for crystallization of minerals in which Li is an essential structural constituent. In the San Diego pegmatites, such high concentrations apparently existed only in the core zones and the pockets.

The influence of the estimated initial 630 ppm Li on the viscosity of the dikes was likely far smaller in comparison with the influence of the ~ 6 wt.% H_2O that would be in the melt at the point of saturation. Even in the core zones where Li_2O may have reached 1 %, its effect would likely have been much smaller. 1 % Li_2O is equivalent to 1.9 mole % in a haplogranite melt, whereas 6 wt% H_2O is equivalent to ~ 18.5 mole %. The addition of 1 wt.% of excess Li to a haplogranite melt lowers the viscosity by about one order of magnitude (Dingwell *et al.*, 1996), but in a peraluminous melt where Li may be complexed with Al in a $Si^{4+} = Al^{3+} + Li^{+}$ substitution, the effect of Li addition is probably smaller. Even if Li exceeded its

charge-balancing role in the melt upon removal of Al by crystallization of the highly peraluminous tourmaline, or if Al was complexed with F in a non-network position in the melt (Giordano *et al.*, 2004; Mysen & Richet, 2005), Li is not expected to have had a drastic effect on the viscosity of the dikes. In comparison, when H_2O is added to a silicate melt, it initially dissolves by forming Al-OH and Si-OH complexes, which depolymerize the tetrahedral network. Viscosity drops by ~ 4.5 orders of magnitude with the addition of only 1 wt.% H_2O to a peraluminous leucogranite melt at 600 °C, and by an additional 6 orders of magnitude with further addition of 5 wt.% H_2O (Romano *et al.*, 2001; Whittington *et al.*, 2004). The decreasing effect of H_2O addition on the viscosity comes from the increasingly greater dissolution of H_2O as a molecular species (Stolper, 1982). Likewise, diffusivities of ions in silicate melts dramatically increase with the addition of only a small amount of H_2O, but less so with further addition of H_2O (Watson, 1994).

Lithium isotope fractionation

A potentially large fractionation of Li-isotopes in any multiphase system is due to the 17 % mass difference between ^{7}Li and ^{6}Li. Presently available data show only very limited Li isotope fractionation during crystallization of high-temperature igneous systems (Tomascak *et al.*, 1999; Magna *et al.*, 2006; Halama *et al.*, 2007) and during vapor-liquid separation in hydrothermal systems (Foustoukos *et al.*, 2004; Liebscher *et al.*, 2007). However, significant fractionation may result from different coordination states of Li in coexisting phases that include multiple minerals, melts, and aqueous fluids in relatively low-temperature granitic systems (Wenger & Armbruster, 1991). In general, ^{6}Li preferentially occupies sites with higher coordination numbers and therefore weaker bonds, whereas ^{7}Li preferentially enters sites with smaller coordination numbers and stronger bonds (Wunder *et al.*, 2007).

Fractionation of Li between minerals and fluids has been experimentally determined only for a limited set of minerals to date. Wunder *et al.* (2006, 2007) found that $\Delta^7Li_{staurolite-fluid} = +1.3$ ‰ and is essentially temperature-independent. $\Delta^7Li_{lepidolite-fluid}$ is approximately –2 ‰ with some temperature dependence in the 350–400 °C range. $\Delta^7Li_{spodumene-fluid}$ is also temperature-dependent, but more negative by about 3 ‰. For all three minerals, the fractionation is insensitive to the Cl content of the fluid, which implies that Li probably forms a tetrahedrally-coordinated hydrated ion $Li(H_2O)_4^+$ instead of a LiCl or LiOH complex. Wunder *et al.* (2007) concluded that equilibrium isotopic fractionation is firstly controlled by Li coordination, with ^{7}Li preferentially incorporated into the phase that allows for a smaller coordination number, and secondly by the Li-O bond length, giving the relationship $\delta^7Li_{staurolite} > \delta^7Li_{lepidolite} > \delta^7Li_{spodumene}$. In staurolite Li substitutes for the divalent cations Fe^{2+}, Mg, and Zn in the tetrahedral sites, in lepidolite Li is octahedrally-coordinated between tetrahedral layers, and in spodumene it occupies the relatively large M2 octahedral site. There are no experimental Li isotope fractionation data involving either tourmaline or melt, but in tourmaline Li occupies the octahedrally-coordinated Y-site and in a peraluminous melt, Li is probably strongly bonded in its charge balancing role with tetrahedrally-coordinated Al^{3+} in a $LiAlSi_3O_8$ complex (Mysen & Richet, 2005). Therefore Li in such a melt should be isotopically relatively heavy.

The results of Wunder *et al.* (2007) involving muscovite are quite different from the results of Lynton et al (2005) who found $\Delta^7Li_{muscovite-fluid}$ to range between +8 and +20 in the 400–500 °C interval. Wunder *et al.* (2007) attributed the discrepancy to the diffusion mechanism that Lynton *et al.* (2005) used to introduce Li into muscovite. Indeed, Teng *et al.* (2006a) ascribed very large variations in δ^7Li of country rocks in the aureole of the Tin Mountain pegmatite to differential diffusion of the two Li isotopes, which underscores that, in addition to the energy of bonds in lattices, kinetic effects may induce transient Li isotope fractionation, which may be preserved in rapidly cooled systems.

There have been no direct measurements of Li isotope fractionation between peraluminous silicate melts and aqueous fluids, but it is expected that Li in a melt should be isotopically heavier because of strong bonds in association with charge balancing of Al that is in tetrahedral coordination. This inference is supported by isotopic compositions of Li in fluid inclusions and host quartz in the Tin Mountain pegmatite in the Black Hills (Teng *et al.*, 2006b). Li in the fluid inclusions has much lower δ^7Li values than Li in the quartz, supporting the inference that ^{7}Li prefers the strong bonds in quartz where it is possibly charge-balancing Al that is incorporated into the quartz structure, and by analogy bonds in high-silica melts over the weaker hydrated bonds in the fluid.

The San Diego pegmatites were systems in which minerals, melts, and aqueous fluids coexisted at various stages of crystallization. Assuming equilibrium, the isotopic composition of Li in tourmaline in the dikes is reflective of the medium from which the tourmaline crystallized. However, Li isotopes may be strongly fractionated by kinetic effects. There is a several permil heterogeneity in δ^7Li even in individual zones of a single pegmatite. Most interesting are the very elevated, > 19 ‰ δ^7Li values of radial tourmalines in both the hanging and lower pegmatite zones. A reason for the elevated values may be that the tourmalines grew when the melt became saturated in the aqueous fluid, at which point Li isotopes were fractionated between the melt and the aqueous fluid with most Li going into the fluid (Fig. 5). If the isotopic composition of Li in tourmaline in each of the zones reflects the relative fractionation of Li isotopes between the melt and the fluid, then the isotopically heavier Li in the pegmatite zone tourmaline is consistent with the expected stronger Li bonds in the melt compared to bonds of hydrated Li in the fluid. The similarity of δ^7Li values in tourmaline that crystallized in the line rock and the pockets is consistent with accumulation of the bulk of melt's initial Li into the pocket fluid, as this would result in little change in the isotopic composition of Li from the initial fluid-undersatured melt to the eventually collected fluid in the pockets. Elbaite rims of pocket tourmalines have lower δ^7Li than their corresponding cores, although one core-rim pair has overlapping analytical errors (Fig. 4b). The lower

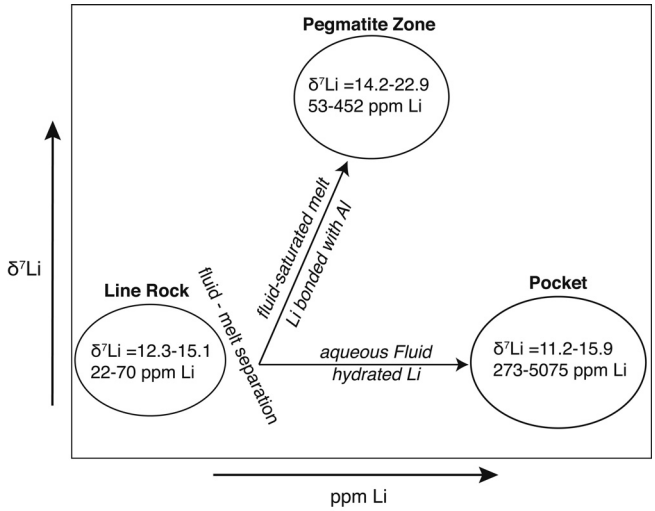

Fig. 5. Schematic diagram illustrating a possible mechanism of producing high δ^7Li tourmalines in pegmatite zones during fluid-melt separation. Because Li is used in charge-balancing with strongly-bonded Al in the silicate melt, the δ^7Li in the melt should be more elevated than δ^7Li in the fluid where Li probably occurs mostly as a hydrated ion (Wunder *et al.*, 2007). Tourmalines crystallizing in equilibrium with the melt and fluid, respectively, may reflect the isotopic fractionation between the melt and the fluid.

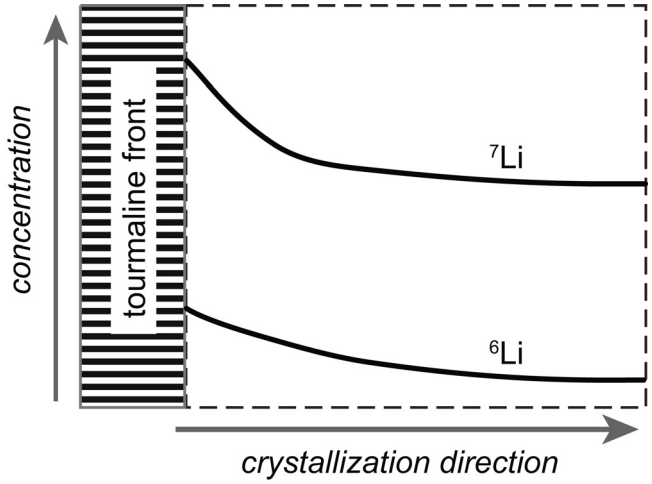

Fig. 6. Schematic diagram illustrating a possible kinetic mechanism of producing high δ^7Li radial tourmalines in pegmatite zones. Because the diffusion of ^{7}Li is slower in the melt than the diffusion of ^{6}Li and when Li is an incompatible element relative to tourmaline, ^{7}Li should become preferentially enriched in a boundary layer ahead of a tourmaline crystal that is growing faster than the rate at which Li diffuses in the melt.

δ^7Li values of the elbaite rims are consistent with crystallization of schorl cores while melt was still present and crystallization of elbaite rims in the presence of the fluid only.

The lack of a systematic increase in δ^7Li across the textural zones of the dikes suggests that there was little influence of tourmaline itself on the isotopic composition of the residual melt during crystallization. Given that both $\Delta^7Li_{spodumene-fluid}$ and $\Delta^7Li_{lepidolite-fluid}$ are both negative, $\Delta^7Li_{tourmaline-melt}$ should be even more negative because Li in tourmaline is in octahedral coordination while in the melt it is associated with tetrahedral Al. However, because the proportion of tourmaline in the line-rock and pegmatite zones is < 8 % and the concentration of Li in the tourmaline is very small, crystallization of tourmaline would have had a negligible effect on the Li isotope ratio in the residual melt. Based on mass-balance calculations, only ~ 2 % of the initial 630 ppm Li is contained in schorl in the line-rocks and the pegmatites zones.

Kinetic effects

A kinetic cause for the elevated δ^7Li values of the radial tourmalines in the pegmatite zones must also be considered, however. The shape of the tourmalines suggests that they grew very rapidly, in which case the Li isotope fractionation may have been kinetically controlled by differential diffusion of Li isotopes at the crystal-liquid (and/or crystal-fluid?) interface. The relative diffusion rates of two isotopes of a given element in a silicate liquid are given by

$$\frac{D_l}{D_h} = \left(\frac{m_h}{m_l}\right)^{\beta}$$

where m is the mass of isotope, "l" stands for the light isotope, and "h" stands for the heavy isotope (Richter *et al.*, 2003). Using basalt-rhyolite melt couples, Richter *et al.* (2003) experimentally determined that $\beta_{Li} \approx 0.215$. This means that ^{6}Li can diffuse substantially faster than ^{7}Li through the melt away from a growing crystal, so that a preferential enrichment of ^{7}Li can potentially occur in the chemical boundary layer ahead of the crystal (Fig. 6), resulting in elevated δ^7Li. The diffusion rate of Li in silicate melts is orders of magnitude faster than the rates of other major and minor cations (Richter *et al.*, 2003). Under conditions of slow mineral growth, homogeneous Li isotope ratios would be expected in the tourmalines. Instead, the observed Li isotope heterogeneity suggests crystallization conditions under which the diffusion of Li in the melt did not keep-up with the rate of tourmaline growth.

Elevated δ^7Li values of pegmatites

The overall elevated δ^7Li values seen in the San Diego pegmatites are similar to the values in the Tin Mountain pegmatite in the Black Hills. δ^7Li values in the associated Harney Peak leucogranite and the host schists of the Tin Mountain pegmatite have δ^7Li values within a few permil of 0, which points to some process that leads to strong Li isotope fractionation during generation of LCT-type pegmatite melts (Teng *et al.*, 2006b). The apparent large fractionation for these relatively low-temperature igneous systems contrasts with the minimal fractionation in

high-temperature igneous systems (Tomascak, 2004). Teng *et al.* (2006b) suggested that elevated δ^7Li values in pegmatite melts could potentially be acquired by crystal-liquid fractionation during crystallization of parental magmas. However, for this process to be effective, a greater amount of Li would have to remain in the crystallized assemblage (parental granite) than in the residual liquid (pegmatite). This is inconsistent with, for example, the relative concentrations of Li in the Harney Peak leucogranite and its potentially residual liquid now represented by the Tin Mountain pegmatite. Li concentrations in the Harney Peak leucogranite range from 10–205 ppm (Teng *et al.*, 2006b).

A possible alternative explanation is that the structure of a hydrous pegmatite melt has more similarity to water than to minerals, and therefore, it incorporates ^{7}Li preferentially over minerals, in a fashion analogous to the large ^{7}Li enrichment in crustal fluids compared to crustal rocks (Tomascak, 2004). As hydrated pegmatite melts pass through the crust from their sources, they may acquire elevated δ^7Li values through rapid Li isotope exchange with the surrounding rocks. Matthews *et al.* (2003) found that the oxygen and especially hydrogen isotopic composition of pegmatite dikes on Naxos, Greece, reflects the isotopic composition of the host rocks, which change in isotopic composition along strike of the dikes. If hydrogen isotopes can be nearly fully exchanged between pegmatite melts and their host rocks, then it is likely that Li isotopes can also be readily exchanged given the fast diffusion rates of Li in silicate liquids (Richter *et al.*, 2003).

Acknowledgements: We are grateful for access provided by Dana and Ken Gochenour to the Cryo-Genie property, Bill Calhoun to the San Diego mine property, and Louis Spaulding, Jr., to the Little Three property. Jeffrey Patterson and Matt Taylor provided guidance around the pegmatite districts and Jim Student helped with sample collection. Carol Nabelek oversaw the ICP-OES analysis. Bill McDonough graciously gave access to JM to conduct analysis in the isotope laboratory at the University of Maryland. The paper benefited from the constructive reviews of Axel Liebscher, Jeffrey Ryan and Ed Grew, and additional comments from Roberta Rudnick. A Feodor-Lynen fellowship to Halama by the Alexander von Humboldt Foundation is gratefully acknowledged. The study was supported by University of Missouri Research Board Grant D3508 and NSF Grant 408564 to Nabelek. Additional funding came from NSF Grant EAR 0606989 to Rudnick and McDonough.

References

Anderko, A. & Pitzer, K.S., (1993): Equation-of-state representation of phase equilibria and volumetric properties of the system NaCl-H_2O above 573 K. *Geochim. Cosmochim. Acta*, **57**, 1657-1680.

Bouman, C., Elliott, T., Vroon, P.Z. (2004): Lithium inputs to subduction zones. *Chem. Geol.*, **212**, 59-79.

Černý, P. (1991): Rare-element granitic pegmatites. Part I: Anatomy and internal evolution of pegmatite deposits. *Geoscience Canada*, **18**, 49-67.

Černý, P. & Ercit, T.S. (2005): The classification of granitic pegmatites revisited. *Can. Mineral.*, **43**, 2005-2026.

Dingwell, D.B., Hess, K.-U., Knoche, R. (1996): Granite and granitic pegmatite melts: volumes and viscosities. *Trans. R. Soc. Edinburgh: Earth Sci.*, **87**, 65-72.

Fenn, P.M. (1977): The nucleation and growth of alkali feldspars from hydrous melts. *Can. Mineral.*, **15**, 135-161.

Fisher, J. (2002): Gem and rare-element pegmatites of southern California. *Mineral. Record*, **33**, 363-407.

Fisher, J., Foord, E.E., Bricker, G.A. (1999): The geology, mineralogy, and history of the Himalaya Mine, Mesa Grande, San Diego County, California. *California Geol.*, 3-17.

Foord, E.E. (1976): Mineralogy and petrogenesis of layered pegmatite-aplite dikes in the Mesa Grande District, San Diego County, California. *Ph.D. Dissertation.* Stanford University.

Foord, E.E., Starkey, H.C., Taggard, J.E., Jr. (1986): Mineralogy and paragenesis of "pocket" clays and associated minerals in complex granitic pegmatites, San Diego County, California. *Am. Mineral.*, **71**, 428-439.

Foustoukos, D.I., James, R.H., Berndt, M.E., Seyfried, W.E., Jr. (2004): Lithium isotopic systematics of hydrothermal vent fluids at the Main Endeavour Field, Northern Juan de Fuca Ridge. *Chem. Geol.*, **212**, 17-26.

Giordano, D., Romano, C., Dingwell, D.B., Poe, B., Behrens, H. (2004): The combined effects of water and fluorine on the viscosity of silicic magmas. *Geochim. Cosmochim. Acta.*, **68**, 5159-5168.

Halama, R., McDonough, W.F., Rudnick, R.L., Keller, J., Klaudius, J. (2007): The Li isotopic composition of Oldoinyo Lengai: Nature of the mantle sources and lack of isotopic fractionation during carbonatite petrogenesis. *Earth Planet. Sci. Lett.*, **254**, 77-89.

Holtz, F., Behrens, H., Dingwell, D.B., Johannes, W. (1995): Water solubility in haplogranite melts: Compositional, pressure and temperature dependence. *Am. Mineral.*, **80**, 94-108.

Jahns, R. H. (1979): Gem-bearing pegmatites in San Diego County, California: The Stewart mine, Pala district, and the Himalaya mine, Mesa Grande district. in "Mesozoic crystalline rocks: Peninsular Ranges batholith and pegmatites, Point Sol ophiolite", P. L. Abbott & V. R. Todd. eds. San Diego State University, San Diego, California, 3-38.

Jahns, R.H. & Burnham, C.W. (1969): Experimental studies of pegmatite genesis: I. A model for the derivation and crystallization of granitic pegmatites. *Econ. Geol.*, **64**, 843-864.

Jahns, R.H. & Tuttle, O.F. (1963): Layered pegmatite-aplite intrusives. *Mineral. Soc. Am. Sp. Pap.*, **1**, 78-92.

Jolliff, B.L., Papike, J.J., Shearer, C.K., Laul, J.C. (1986): Tourmaline as a recorder of pegmatite evolution: Bob Ingersol pegmatite, Black Hills, South Dakota. *Am. Mineral.*, **71**, 472-500.

Kalt, A., Schreyer, W., Ludwig, T., Prowatke, S., Bernhardt, H., Ertl, A. (2001): Complete solid solution between magnesian schorl and lithian excess-boron olenite in a pegmatite from the Koralpe (eastern Alps, Austria). *Eur. J. Mineral.*, **13**, 1191-1205.

Kampf, A.R., Gochenour, K., Clanin, J. (2003): Tourmaline: discovery at the Cryo-Genie mine, San Diego County, California. *Rocks and Minerals*, **78**, 156-163.

Liebscher, A., Meixner, A., Romer, R.L., Heinrich, W. (2007): Experimental calibration of the vapour–liquid phase relations and lithium isotope fractionation in the system H_2O–LiCl at 400. *Geofluids*, **7**, 1-7.

London, D. (1986a): Magmatic-hydrothermal transition in the Tanco rare-element pegmatite: Evidence from fluid inclusions and phase-equilibrium experiments. *Am. Mineral.*, **71**, 376-395.

– (1986b): Formation of tourmaline-rich gem pockets in miarolitic pegmatites. *Am. Mineral.*, **71**, 396-405.

– (1992): The application of experimental petrology to the genesis and crystallization of granitic pegmatites. *Can. Mineral.*, **30**, 499-540.

London, D., Hervig, R.L., Morgan, G.B., VI (1988): Melt-vapor solubilities and elemental partitioning in peraluminous granite-pegmatite systems: experimental results with Macusani glass at 200 MPa. *Contrib. Mineral. Petrol.*, **99**, 360-373.

Lynton, S.J., Walker, R.J., Candela, P.A. (2005): Lithium isotopes in the system Qz-Ms-fluid: An experimental study. *Geochim. Cosmochim. Acta.*, **69**, 3337-3347.

Magna, T., Wiechert, U., Grove, T.L., Halliday, A.N. (2006): Lithium isotope fractionation in the southern Cascadia subduction zone. *Earth Planet. Sci. Lett.*, **250**, 428-443.

Matthews, A., Putlitz, B., Hamiel, Y., Hervig, R.L. (2003): Volatile transport during the crystallization of anatectic melts: oxygen, boron and hydrogen stable isotope study on the metamorphic complex of Naxos, Greece. *Geochim. Cosmochim. Acta*, **67**, 3145-3163.

Morgan, G.B., VI & London, D. (1999): Crystallization of the Little Three layered pegmatite-aplite dike, Ramona District, California. Contrib. *Mineral. Petrol.*, **136**, 310-330.

Moriguti, T., Nakamura, E. (1998): High-yield lithium separation and the precise isotopic analysis for natural rock and aqueous samples. *Chem. Geol.*, **145**, 91-104.

Mysen, B.O., and Richet, P. (2005): Silicate glasses and melts, properties and structure. Elsevier, Amsterdam, 544 p.

Nabelek, P.I. (2007): A kinetic model for crystallization of granitic pegmatites at very low temperatures. *6th Hutton Symposium*, 150-151.

Norton, J.J. (1994): Structure and bulk composition of the Tin Mountain Pegmatite, Black Hills, South Dakota. *Econ. Geol.*, **89**, 1167-1175.

Qi, H.P., Taylor, P.D.P., Berglund, M., De Bievre, P. (1997): Calibrated measurements of the isotopic composition and atomic weight of the natural Li isotopic reference material IRMM-016. *Int. J. Mass Spectrom. Ion Process.*, **171,** 263-268.

Richter, F.M., Davis, A.M., Depaolo, D.J., Watson, E.B. (2003): Isotope fractionation by chemical diffusion between molten basalt and rhyolite. *Geochim. Cosmochim. Acta.*, **67**, 3905-3923.

Rockhold, J.R., Nabelek, P.I., Glascock, M.D. (1987): Origin of rhythmic layering in the Calamity Peak satellite pluton of the Harney Peak Granite, South Dakota: The role of boron. *Geochim. Cosmochim. Acta.*, **51**, 487-496.

Romano, C., Poe, B., Mincione, V., Hess, K.U., Dingwell, D.B. (2001): The viscosities of dry and hydrous $XAlSi_3O_8$ (X = Li, Na, K, $Ca_{0.5}$, $Mg_{0.5}$) melts. *Chem. Geol.*, **174**, 115-132.

Rudnick, R.L., Tomascak, P.B., Njo, H.B., Gardner, L.R. (2004): Extreme lithium isotopic fractionation during continental weathering revealed in saprolites from South Carolina. *Chem. Geol.*, **212**, 45-57.

Schreyer, W., Wodara, U., Marler, B., van Aken, P.A., Seifert, F., Robert, J.-L. (2000): Synthetic tourmaline (olenite) with excess boron replacing silicon in the tetrahedral site: I. Synthesis conditions, chemical and spectroscopic evidence. *Eur. J. Mineral.*, **12**, 529-541.

Sirbescu, M.C. & Nabelek, P.I. (2003a): Crystallization conditions and evolution of magmatic fluids in the Harney Peak Granite and associated pegmatites, Black Hills, South Dakota – Evidence from fluid inclusions. *Geochim. Cosmochim. Acta.*, **67**, 2443-2465.

–,– (2003b): Crustal melts below 400 °C. *Geology*., **31**, 685-688.

Sirbescu, M.C., Hartwick, E.E., Student, J.J. (2008): Rapid crystallization of the Animikie Red Ace Pegmatite, Florence County, Northeastern Wisconsin: Inclusion microthermometry and conductive-cooling modeling. *Contrib. Mineral. Petrol.*, in press.

Stern, L.A., Brown, G.E., Bird, D.K., Jahns, R.H., Foord, E.E., Shigley, J.E., Spaulding, L.B., Jr. (1986): Mineralogy and geochemical evolution of the Little Three pegmatite-aplite layered intrusive, Ramona, California. *Am. Mineral.*, **71**, 406-427.

Stolper, E. (1982): The speciation of water in silicate melts. *Geochim. Cosmochim. Acta.*, **46**, 2609-2620.

Symons, D.T.A., Walawender, M.J., Smith, T.E., Molnar, S.E., Harris, M.J., Blackburn, W.H. (2003): Palomagnetism and geobarometry of the La Posta pluton, California. in: *Geol. Soc. Am. Spec. Pap. 374: Tectonic Evolution of Northwestern Mexico and the Southwestern USA*. S.E. Johnson, S.R. Paterson, J.M. Fletcher, D.L. Kimbrough, A. Martin-Barajas eds., 93-116.

Teng, F., McDonough, W.F., Rudnick, R.L., Dalpé, C., Tomascak, P.B., Chappell, B.W., Gao, S. (2004): Lithium isotopic composition and concentration of the upper continental crust. *Geochim. Cosmochim. Acta.*, **68**, 4167-4178.

Teng, F., McDonough, W.F., Rudnick, R.L., Walker, R.J. (2006a): Diffusion-driven extreme lithium isotopic fractionation in country rocks of the Tin Mountain pegmatite. *Earth Planet. Sci. Lett.*, **243**, 701-710.

Teng, F., McDonough, W.F., Rudnick, R.L., Walker, R.J., Sirbescu, M.C. (2006b): Lithium isotopic systematics of granites and pegmatites from the Black Hills, South Dakota. *Am. Mineral.*, **91**, 1488-1498.

Thomas, A.V., Bray, C.J., Spooner, E.T.C. (1988): A discussion of the Jahns-Burnham proposal for the formation of zoned granitic pegmatites using solid-liquid-vapour inclusions from the Tanco Pegmatite, S.E. Manitoba, Canada. *Trans. R. Soc. Edinburgh: Earth Sci.*, **7**, 299-315.

Thomas, R. & Klemm, W. (1997): Microthermometric study of silicate melt inclusions in Variscan granites from SE Germany: Volatile contents and entrapment conditions. *J. Petrol.*, **38**, 1753-1765.

Thomas, R., Webster, J.D., Heinrich, W. (2000): Melt inclusions in pegmatite quartz: complete miscibility between silicate melts and hydrous fluids at low pressure. *Contrib. Mineral. Petrol.*, **139**, 394-401.

Todd, V.R., Shaw, S.E., Hammarstrom, J.M. (2003): Cretaceous plutons of the Peninsular Ranges batholith, San Diego and westernmost Imperial Counties, California: Intrusion across a Late Jurassic continental margin. *Geol. Soc. Am. Spec. Pap.*, **374**, 185-235.

Tomascak, P.B. (2004): Developments in the understanding and application of lithium isotopes in the Earth and planetary sciences. *Rev. Mineral. Geochem.*, **55**, 153-195.

Tomascak, P.B., Tera, F., Helz, R.T., Walker, R.J. (1999): The absence of lithium isotope fractionation during basalt differentiation; new measurements by multicollector sector ICP-MS. *Geochim. Cosmochim. Acta*, **63**, 907-910.

Walawender, M.J., Gastil, R.G., Clinkenbeard, J.P., McCormick, W.V., Eastman, B.G., Wernicke, R.S., Wardlaw, M.S., Gunn, S.H., Smith, B.M. (1990): Origin and evolution of the zoned La Posta-type plutons, eastern Peninsular Ranges batholith, southern and Baja California. in "The nature and origin of Cordilleran magmatism", J. L. Anderson. ed. Boulder, Colorado, 1-18.

Walker, R.J., Hanson, G.N., Papike, J.J., O'neil, J.R., Laul, J.C. (1986): Internal evolution of the Tin Mountain pegmatite, Black Hills, South Dakota. *Am. Mineral.*, 71, 440-459.

Watson, E.B. (1994): Diffusion in volatile-bearing magmas. *Rev. Mineral.*, **30**, 371-411.

Webber, K.L., Simmons, W.B., Falster, A.U., Foord, E.E. (1999): Cooling rates and crystallization dynamics of shallow level pegmatite-aplite dikes, San Diego County, Califronia. *Am. Mineral.*, **84**, 708-717.

Webster, J.D., Holloway, J.R., Hervig, R.L. (1989): Partitioning of lithophile trace elements between H_2O and H_2O + CO_2 fluids and topaz rhyolites. *Econ. Geol.*, **84**, 116-134.

Wenger, M. & Armbruster, T. (1991): Crystal-chemistry of lithium–oxygen coordination and bonding. *Eur. J. Mineral.*, **3**, 387-399.

Whittington, A., Richet, P., Behrens, H., Holtz, F., Scaillet, B. (2004): Experimental temperature-X(H_2O)-viscosity relationship for leucogranites and comparison with synthetic silicic liquids. *Trans. R. Soc. Edinburgh: Earth Sci.*, **95**, 59-71.

Wunder, B., Meixner, A., Romer, R.L., Heinrich, W. (2006): Temperature-dependent isotopic fractionation of lithium between clinopyroxene and high-pressure hydrous fluids. *Contrib. Mineral. Petrol.*, **51**, 112-120.

Wunder, B., Meixner, A., Romer, R.L., Feenstra, A., Shettler, G., Heinrich, W. (2007): Lithium isotope fractionation between Li-bearing staurolite, Li-mica and aqueous fluids: An experimental study. *Chem. Geol.*, 238, 277-290.

Received 12 November 2007
Modified version received 28 February 2008
Accepted 29 February 2008